

# An investigation of thermal energy storage for industrial heat waste recovery: Storing heat waste into a ground TES system for a ship's diesel engine

Hafiz M K U Haq, Birgitta J. Martinkauppi, Erkki Hiltunen

Department of Energy Technology

University of Vaasa

Wolffintie 34 65200 Vaasa

Finland

Hafiz.haq@uva.fi,

Bigitta.martinkauppi@uva.fi,

Erkki.hiltunen@uva.fi

*Abstract:* - Investigating industrial heat waste storage system consists of analysis of the standard thermal energy storage (TES) capacity and the ability to deliver renewable energy into a building's heating system. This purpose was achieved with the establishment of Vaasa Energy Business and Innovation Center (VEBIC) lab in Finland to promote energy business in the country, one of the features of the lab is to test and research on Wärtsilä's diesel engine for ships. This engine produces ultra-exhaustion heat which is planned to be stored in a ground TES. This heat waste is injected at the input to test the validity of TES. Five models of TES is developed based on the energy demand of the lab. TES configuration includes 9 boreholes with varying depth of 40, 100, 150, 200, and 250 meters. Input signal is applied at these models to estimate an appropriate size of TES for given building. TES of 250 meters depth is found to be an appropriate size for VEBIC lab. Heat transfer in the ground is calculated by varying volumetric flow rate from 0.05 to 3.0 liter per second of the carrier fluid. Range of 0.05 to 2.0 liter per second is found to be appropriate for the given case. A series configuration of 4 boreholes is shown to satisfy the space heating demand of the given building.

*Key-Words:* - Industrial waste recovery, Thermal energy storage, Heat exchange in boreholes, Surface temperature change, Heating demand.

## 1 Introduction

TESs may be classified into two categories. One classification is based on loading energy storage while second is heat capacity to be delivered into a given building. This paper deals with both categories in which an industrial waste heat source is selected to charge a TES and deliver this energy to a building's heating system. The intensity of heat source may determine the size of the TES. A comparative study is conducted by developing models of TES and simulating with input signal of industrial heat waste. Energy stored in the TES should be sufficient to meet the heating demand of a test building after subtracting the losses. It means, the quality of a TES limits available energy for a building. A good quality TES is properly insulated as well as reduces heat losses of distribution system, increases the efficiency, and limits cost. This study investigates a periodic heat waste input signal applied at TES. Kandiah and Lightstone (2016)

investigated a heat storage of 35x35 meters area with 30 meters of depth and 2.5 meters distance between boreholes, boreholes were used in conjunction with a buffer tank which accounted for the amount of energy difference between collection and deposit into the borehole fields. Heat losses of the tank were reduced by burying the tank into the ground. Long term performance of energy stored and energy extracted simulated over a period of 20 years with predicted efficiency of borehole thermal energy system was about 50%. Location of a ground heat storage influence its efficiency. Performance of a solar district heating system differ under the influence of location change [4]. TRNSYS was used to conduct simulation of five countries and reported the efficiency of the borehole thermal energy system. Seasonal fraction evidently increased to 90% after five years of operation. Data was compared with the Drake landing solar community project [6]. It pointed out that low temperature heating systems can significantly increase the solar

fraction. Seasonal performance of a combined heat and power plant performance reported to be 90% after 4 years of operation [3]. Simulations was performed using TRNSYS over a period of 5 years. Temperature variation of the ground was presented with regards to the input and output signals. Energy injected into the heat storage was presented to be twice the amount of energy extracted from the system. Experimental study of optimization of borehole heat storage from combined heat and power production in which long term recovery of 65% of heat stored was predicted [13]. Temperature of borehole increased to 75 °C from 40 °C. Model domain assumed a surface area of 1139x765 meters using FEFLOW. Unique configuration of borehole heat exchanger presented to improve heat transfer [17]. Boreholes were configured so that vertical probes immersed in an artificial fluid contained in a case separated from the ground by the usual fitting material. This lead to an increase heat transfer within boreholes, induced natural convection in the annulus between the protection system and the vertical probes. Effect at the depth of boreholes and material property variation influence the ground temperature concealed with borehole heat exchangers [19]. Experimental measurements compared with various models of borehole heat exchanger to study heat flow in a conductive media. Results indicated that heat exchange rate per unit depth of borehole varied with depth in the layers of the ground. Variation in the heat exchange rate over depth showed the anomaly in the lower portions of the ground. Other parameters take part in the heat rate may include thermal load, performance factor and load variation. These parameters were analyzed with a reference data set for validation [7]. Reference data included water temperature, flowrate and power consumption. Validated example presented with experimental data. Cooling demand was predominant over heating demand in the mentioned study. Small scale configuration with an area of 2x3 meters with a 3 meters of borehole separation along with 50 meters depth, was suggested with an optimization technic in simulation of seasonal solar-driven storage system [8]. This demonstrated the sorption process which allowed enhanced operation modes. System was modeled using TRNSYS which include high temperature solar collector loop, heat exchanger, hot water store, buffer tank, condenser, and sorption stores. This study presented a conclusive demonstration of all the component may be required to build a heating system. A network based method was theorized to optimize the configuration of heat storage [1]. Heat storage was configured in a series connection.

System was generalized with an input and an output of the borehole field and few elements such as heat exchanger and mass flowrate of the pump. Borehole field part was separately computed with so-called “g-function”. The rest of the circuit formed a series connection which provided heat transfer. Borehole field was solved with three possible modes. First depicted separate zones for injection and extraction, second presented a mixed zone for injection and extraction, and the third revealed only extraction zone. There has been so much focus on combine heat and power that include the part of thermal energy storage for either district use or an individual building. Flexibility for this kind of system may be an important aspect to raise questions. The nature of energy system on the supply side investigated to determine the theoretical flexibility of combined heat and power system [18]. Flexibility was calculated with the approach of system through delayed or forced operation mode. It was claimed that flexibility has a drastic effect on thermal energy storage as a central unit. Another study presented modelling and optimization of combined heat and power for district heating system with renewable energy production [10]. The main objective of the mentioned study was to reduce the overall costs of the net acquisition of heat and power in deregulated power market. Charging and discharging of heat load studied with solar irradiation. Thermal storage percentage for the months of January and July were plotted. Another central solar heating plant investigated in Germany with seasonal heat storage to reduce carbon dioxide emission and obtain 50% or more solar fraction [5]. Study presented a comprehensive account of different types of heat storage. Analytical model for a ground heat exchanger with ground water flow was investigated [11]. Multiple layers of ground can be consider in the mentioned study. Mixed arrangement of a borehole system with a heat pump was presented [12]. An inquiry of TES is elaborated in the next section. The simulation setting and input parameters are presented respectively. Heat rate during charging operation is calculated. In the following sections, heat demand of a test building case is roughly estimated, follow with heat loss in the ground and heat extraction process, and finally heat capacity of TES is illustrated meeting the heat demand of the test building.

## 2 System description

VEBIC lab is subjected to different tests on ship’s diesel engine. These massive engines have a high exhaust capability. System to be simulated, is depicted in Fig. 1. Exhaustion of diesel engine is

simulated and stored into TES. TES is placed under a test building, which is essentially a heat source of the heating system of building. An auxiliary heating device is placed to fulfill an alternate condition of heat source. Occasional testing of diesel engine produces in heat source signal which is used as input of the TES but the intensity of exhaust signal reportedly recorded very high so that heat exchanger would stabilize the input signal for TES. TES consists of 9 boreholes which may be used simultaneously in a series manner or otherwise, an individual borehole may be selected to store heat energy. Distance between exhaust of diesel to heat exchanger is about 200 meters.

## 2.1 Input signal

Input signal is an essential element in simulating the TES, as the area of TES may be determined by the amount of energy to be injected into TES. For the purpose of this study, input signal was selected based on the exhaust information given, depicted in Fig. 2. An hourly periodic signal for a time period of one month was created, starts at 0 hour with a temperature of 6 °C goes up to 90 °C at the hour 4<sup>th</sup>. Peak of the signal return back to 6 °C by hour 10<sup>th</sup> which remains until 24<sup>th</sup> hour. This signal was suggested for one day operation which continues for a month in Fig. 2. Rest of the simulations required this input signal which in case of contradiction to the experimental measurements, would be changed later on to generate accurate results of the TES.

## 2.2 Modeling TES

Borehole depth and the number of boreholes are the prerequisite of TES in this study, the depth and the number of boreholes were decided early on, to be 9 boreholes with a depth of 250 meters. Research question in this scenario stated as “What would be the thermal response of the ground if the depth of boreholes were to be altered?” and how much power would be transferred to the TES along with the different depths. In response to that question, modeling and simulations were made to produce thermal response of the TES and analyze the best depth. Five models were made of the TES, consisting borehole depths of (40, 100, 150, 200, 250) meters. Model of the TES is presented in Fig. 3. Comsol was used to create models and simulations. Connections of the boreholes showing the possible configuration of the TES in 2D and 3D. In 40 meters configuration, distance between boreholes were selected to be 2.5 meters. The rest of the models implemented with a 5 meters borehole to borehole distance. Configuration chosen to be same in all of the models, the only useable difference was

of the depth. Simulations were arranged so that input signal shown in Fig. 2 applied at the input leg of the TES presented in Fig. 3. Distance between legs of the boreholes was assumed to be 110 millimeters. For the purpose of simulation, properties of water were assumed in the simulation flowing through the borehole’s connections. Material of the ground were assumed to be metamorphic rock. Parameters used in this simulations are presented in Table 1.

Table 1. Parameters used in the simulations.

Parameter	Symbol	Value
Radius of TES	$r_g$	12 (m)
Depth of TES	$L$	40, 100, 150, 200, 250 (m)
Distance between boreholes	$d_g$	2.5, 5 (m)
Leg to leg pipe distance	$D$	110 (m)
Flow rate	$q$	1 (l/s)
Ground thermal conductivity	$k_g$	3.4 (W/m·K)
Initial ground temperature	$T_0$	6 (°C)
Surface temperature	$T_{sur}$	5 (°C)
Boundary temperature of ground	$T_g$	7 (°C)
Inner pipe diameter	$d_i$	35.2 (mm)
Pipe thermal conductivity	$k_p$	0.4 (W/m·K)

Injection process is roughly illustrated in Fig. 4, in which y-axis of the input signal represents a temperature in Kelvin scale. As soon as the input signal applied at the TES, fluid flow through heat exchanger pipes dissipating heat energy into the ground before it comes out from the other end. The amount of heat transfer depends on few constraints such as flow rate of the fluid, depth of the heat exchanger and thermal properties of the fluid and ground. Simulations were set up for a period of one

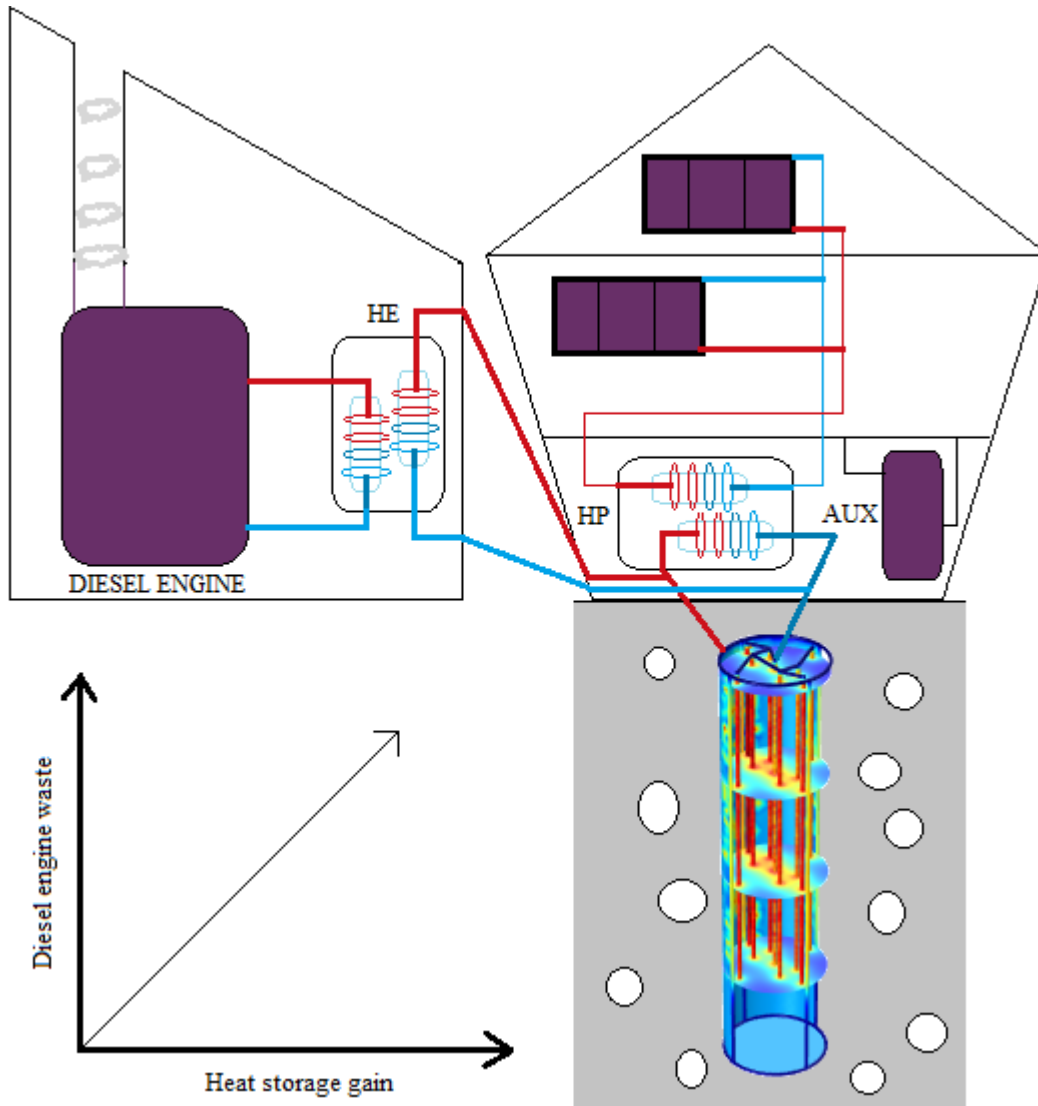


Figure 1. An illustration of the system. Diesel engine is connected with a heat exchanger, storing heat energy into a TES. TES then supply heat energy to a building. Graph suggests that energy gain into TES is proportional to energy waste from diesel engine.

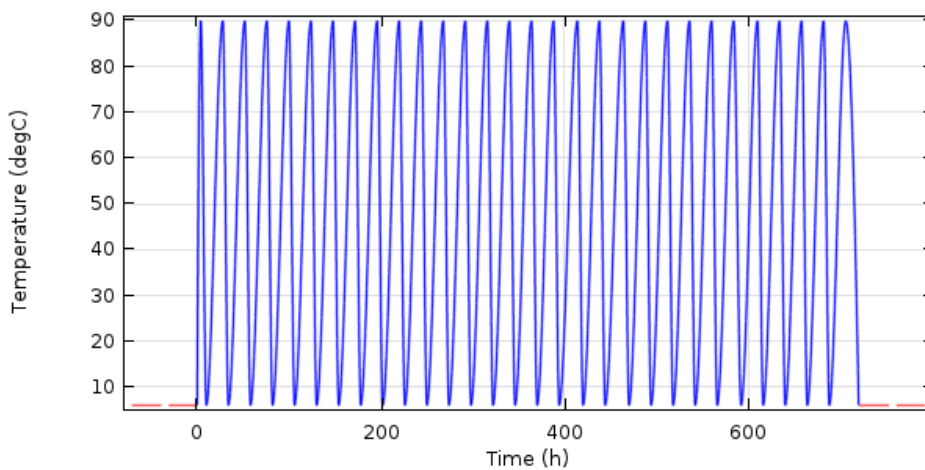


Figure 2. Hourly input signal. Simulation time duration is set to be 720 hours.

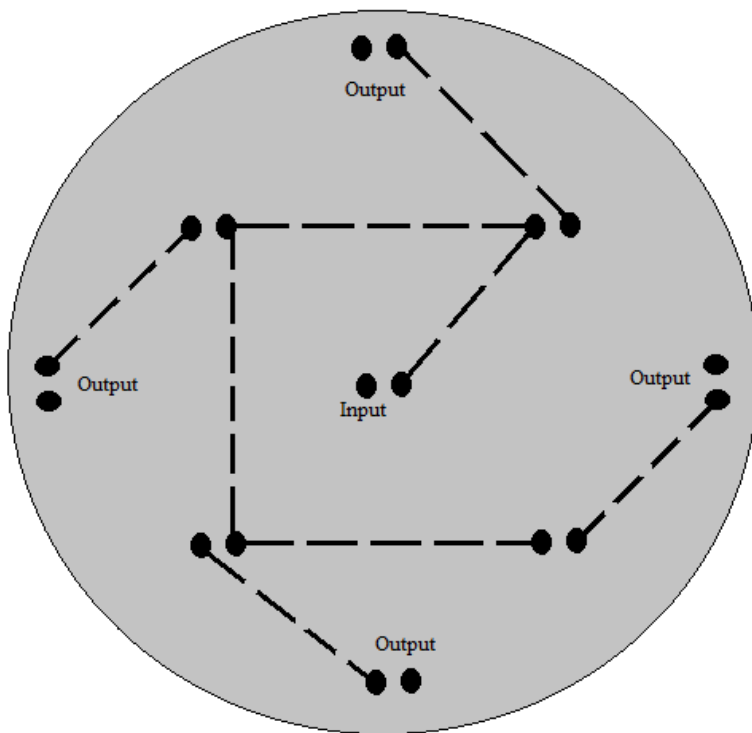


Figure 3. Model of borehole TES. Series connection depicts the starting and ending points of the connection. There are four output points depicted along with one input point. Configuration can be changed for another setting and energy demand.

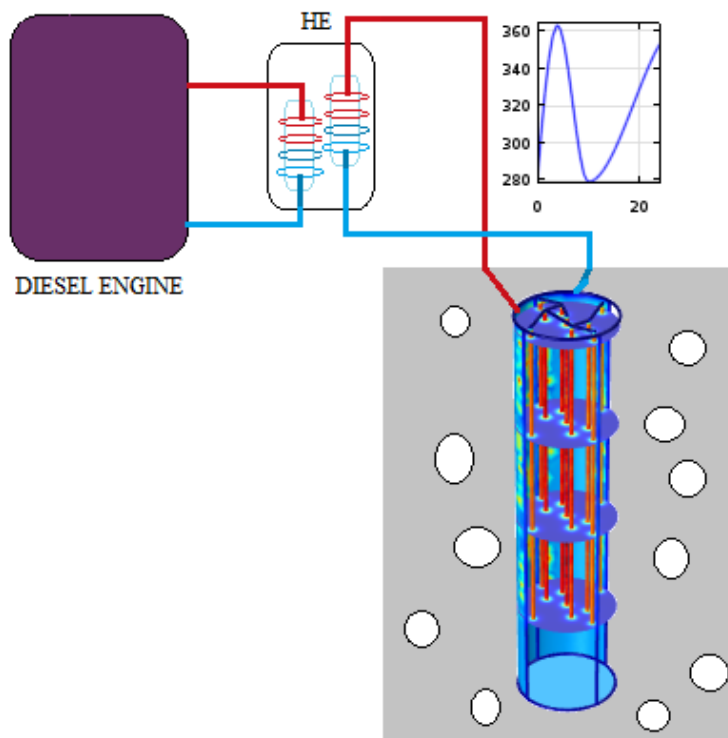


Figure 4. Charging TES. Input signal to the TES interpreted in Kelvin scale. Red line shows hot carrier fluid entering TES while blue line shows cold carrier fluid returning from TES.

month. Power absorbed by the ground or the heat transfer rate is presented in Fig. 5. Series connection presented in Fig. 3 does not strictly bound the experimental strategy. It may be changed based on the temperature measurement of individual boreholes and whichever one provides better thermal response. There are four outputs shown in Fig. 3, either these points will combine together in a series connection or use individually, depending on the heat demand of the building. Heat transfer to the ground is determined by considering one of the output leg temperature, calculated with a simple formula stated as:

$$Q = mc_p(T_{in} - T_{out}) \quad (1)$$

Where,  $Q$  (W) is heat transfer or the amount of power absorbed by the TES,  $m$  (kg/s) is mass flow rate of the fluid,  $C_p$  (J/kg.K) is heat capacity of the fluid, and  $T$  ( $^{\circ}\text{C}$ ) is temperature at the input or output. Five plots were made for five simulations of TES varied in terms of depth in Fig. 5. In the first two plots of 40 and 100 meters, heat rate varies constantly as the input signal varied with time. Small depth of TES showed large variation because fluid did not stay long enough to transfer much heat energy. Rest of the three plots of 150, 200 and 250 meters TES showed steady change in the heat rate giving fluid enough time to transfer heat energy to the ground. The maximum heat transfer presented were found identical in five simulated models, the difference projected in the fluctuations of the pulse found more stable in the 250 meters TES case. Maximum temperature among four output of the 40 meters TES found to be between  $40^{\circ}\text{C}$  to  $45^{\circ}\text{C}$ . Output temperature of the 100 meters TES is more stable than 40 meters TES gave fluid enough time to heat transfer into the ground, maximum output temperature found to be  $18^{\circ}\text{C}$  to  $26^{\circ}\text{C}$ . For 150 meters TES, maximum output fluid temperature calculated to be  $15^{\circ}\text{C}$  to  $20^{\circ}\text{C}$ . Decrease in the output temperature means more heat is transferred into the ground occurred and naturally, the more time fluid circulates underground, the more heat transfer takes place. Maximum output temperature of 200 meters TES calculated to be  $11^{\circ}\text{C}$  to  $14^{\circ}\text{C}$  and at last, 250 meters TES output  $8^{\circ}\text{C}$  to  $9^{\circ}\text{C}$  maximum output temperature. It is more relevant in our case to present ground temperature of TES so to find out the amount of temperature rise in the ground after one month of operation. The initial temperature of the ground assumed to be  $6^{\circ}\text{C}$ . Ground temperature is depicted in Fig. 6 after the operation of one month. As mentioned previously, five consecutive models were made based on depth

of TES. Temperature of the ground after one month was taken from the middle of the TES ground presented in Fig. 6(a). 40 meters TES ground temperature is depicted in Fig. 6(b) in which temperature of the ground go as high as  $30^{\circ}\text{C}$  and the rest of the ground temperature rose from  $6^{\circ}\text{C}$  to  $15^{\circ}\text{C}$ . Ground temperature of 100 and 150 meters in Figs. 6(c-d) TESs does not show a significant rise compare to 40 meters TES. Maximum temperature remains about  $30^{\circ}\text{C}$  but in fewer places and minimum temperature rose up to  $10^{\circ}\text{C}$ . Temperature of 200 and 250 meters in Figs. 6(e-f) TESs showed a gradual increase up to maximum of  $25^{\circ}\text{C}$  and minimum of about  $10^{\circ}\text{C}$ . Ground temperature in these five simulations presents an opportunity to compare between different TES depths and analyze a favorable conclusion based on given scenario. To recall, simulation time period chose to be only one month. In practical case, it would have to go round the year. The intensity of the heat energy to be injected into the ground would suggest a 250 meters TES. Ground temperature of 250 meters TES resulted to be significant enough to use in our scenario. Control of heat transfer of 250 meters TES may be done by varying the volumetric flow rate of the fluid circulation. In all of the previous simulations, volumetric flow rate assumed to be always 1 (l/s). It may be important to point out that heat rate fluctuates with the variation in flow rate of the fluid. To demonstrate that effect, six simulations were made with flow rate variation depicted in Fig. 7. Choosing carefully, 0.05 (l/s) to 3 (l/s) flow rate assumed. From 0.05 (l/s) to 2 (l/s), the stability of the heat rate contained. Flow rate of 2.5 (l/s) and 3 (l/s) found to be high enough to create fluctuations of undesired nature. Flow rate may vary from time to time based on the intensity of the heat source. High intensity input signal may require small flow rate so the stability of heat rate can be maintained. Thermal response of 250 meters TES with flow rate variation is presented in Table 2. Output temperature represents carrier fluid output temperature. Average temperature of the ground is observed in all simulation varying with flow rate.

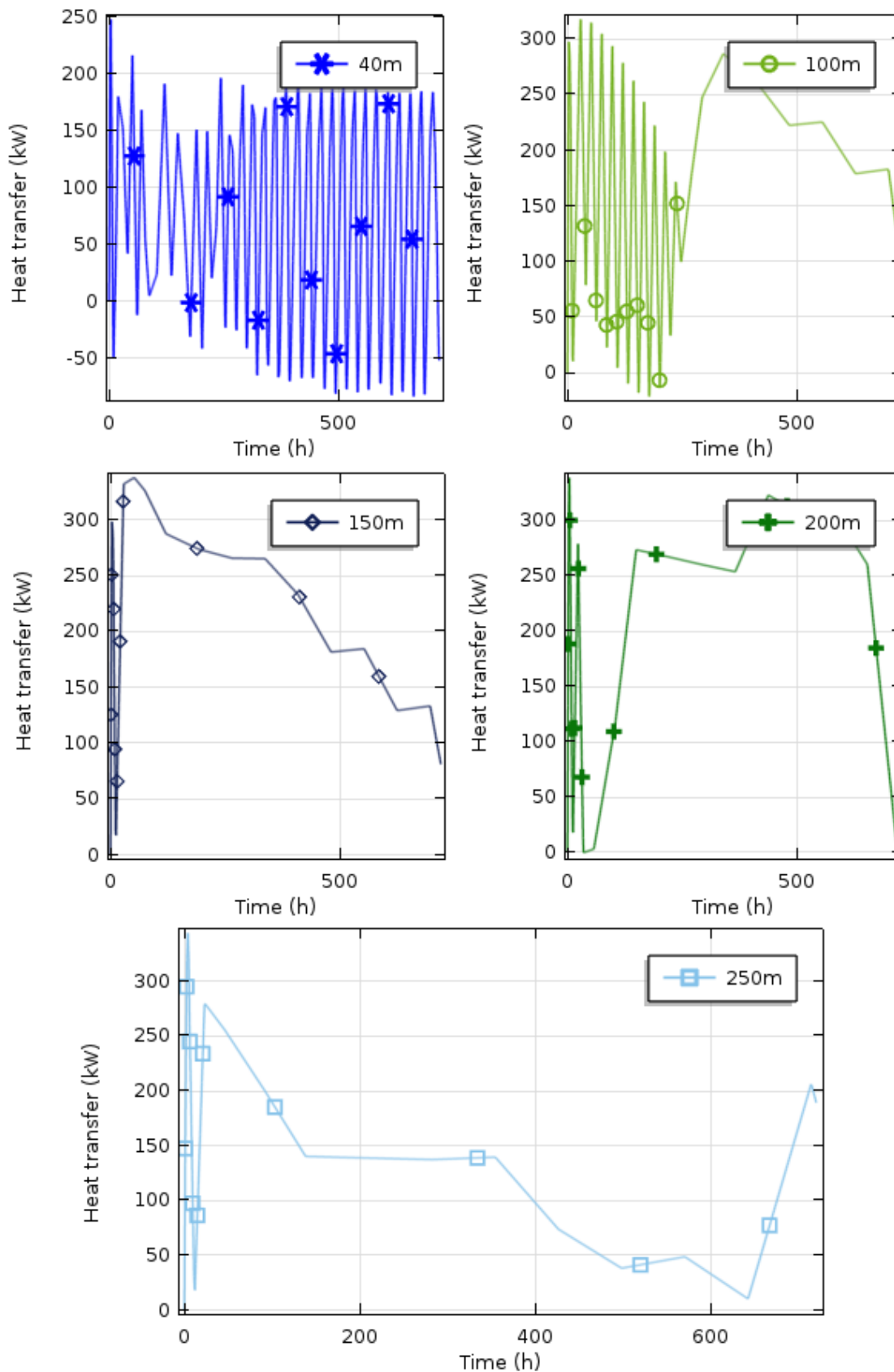


Figure 5. Heat transfer for time period of one month with various depths of TES.

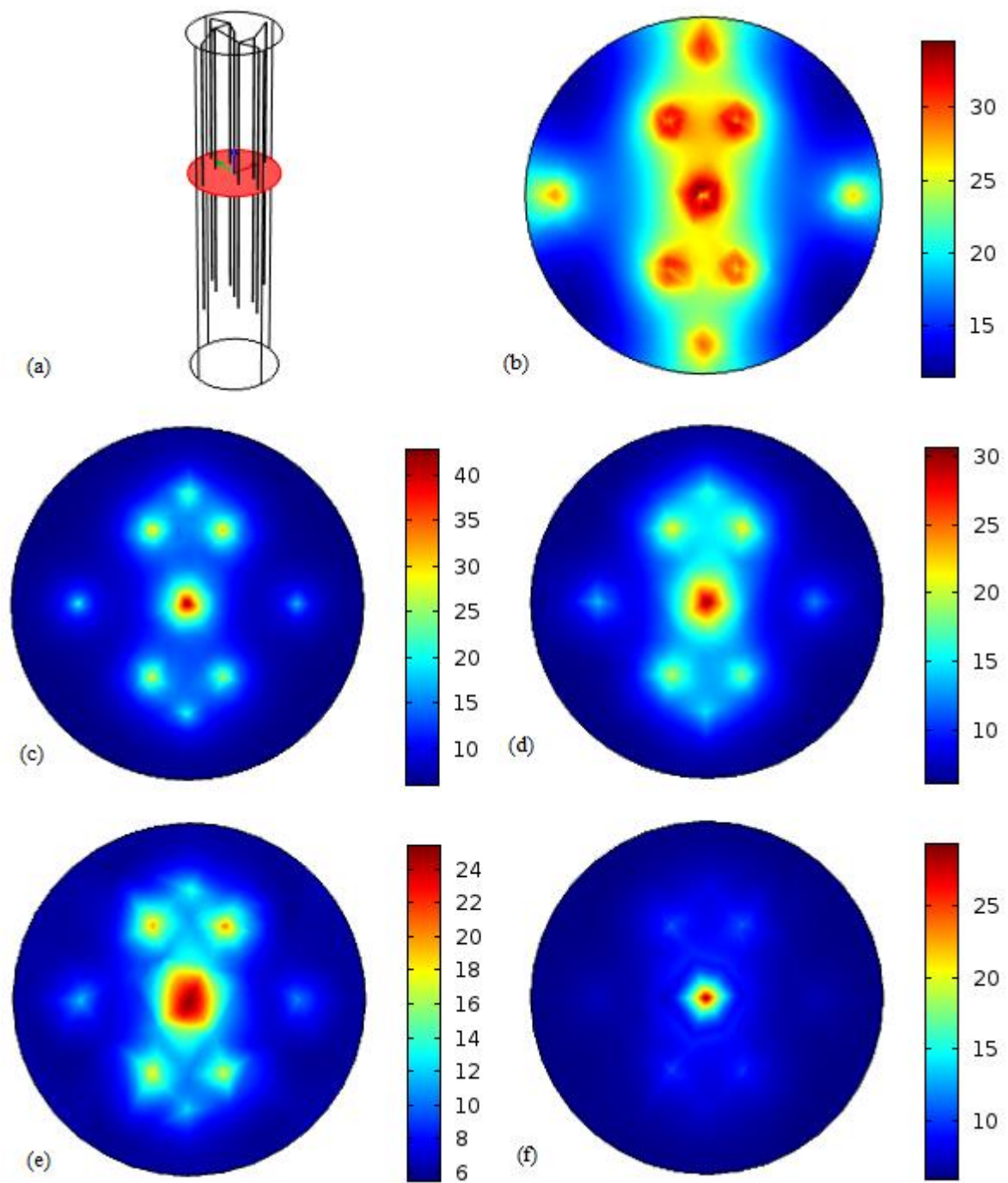


Figure 6. Ground surface temperature after one month of operation. (a) Represents the surface at which 2D surface temperature plotted. (b) 40 m TES. (c) 100 m TES. (d) 150 m TES. (e) 200 m TES. (f) 250 m TES.

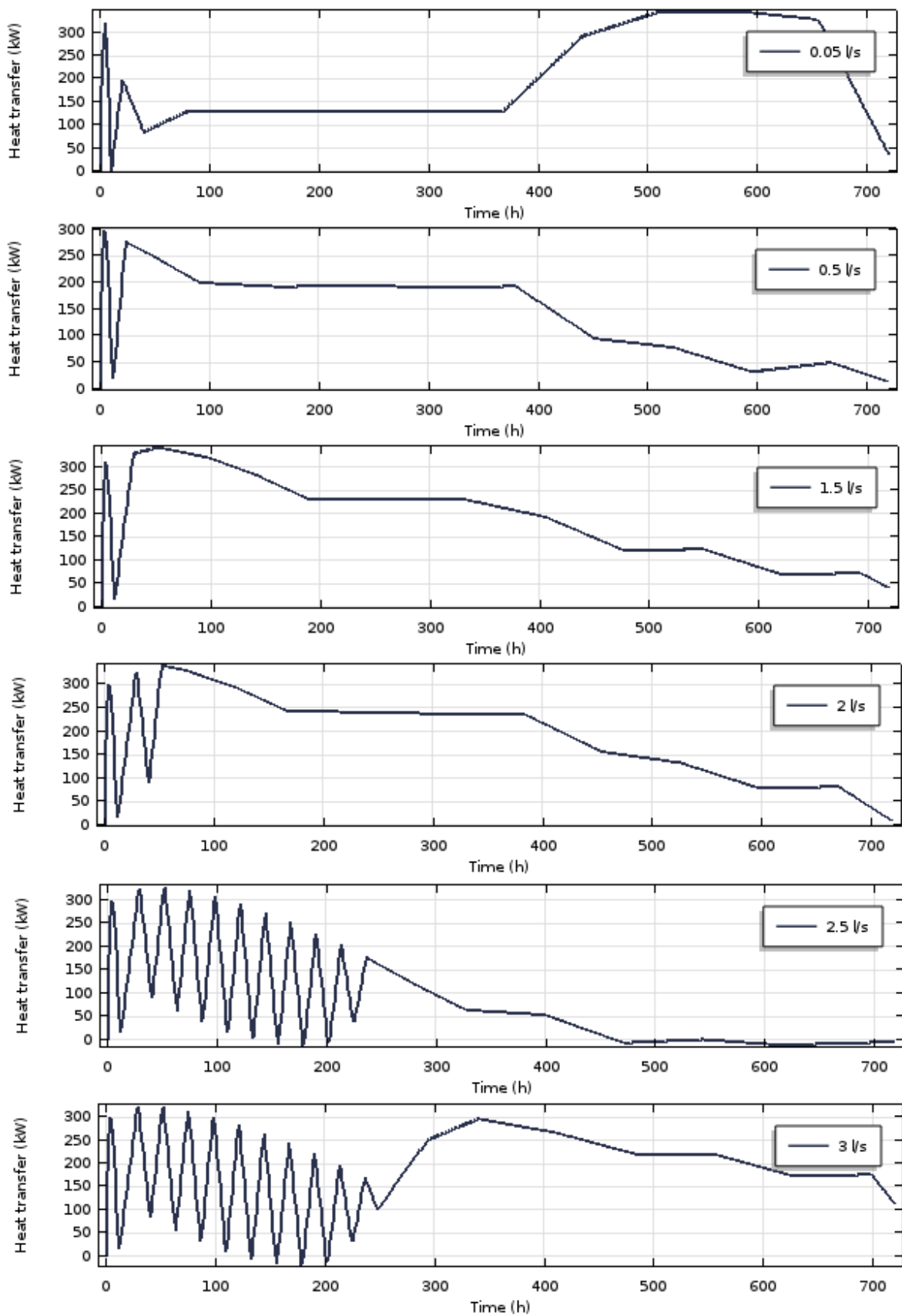


Figure 7. Heat transfer of 250 m TES with variation of volumetric flow rate.

Table 2. Variation at the output and average ground temperature with flow rate in 250 meters TES.

Flow rate (l/s)	$T_{1out(max)}$ ( $^{\circ}C$ )	$T_{2out(max)}$ ( $^{\circ}C$ )	$T_{3out(max)}$ ( $^{\circ}C$ )	$T_{4out(max)}$ ( $^{\circ}C$ )	$T_{ground(avg)}$ ( $^{\circ}C$ )
0.05	6	5.9	5.8	5.8	8
0.5	9	8.4	8.3	7.5	9
1.5	14	13	13	12	13
2	17	16	16	14	10
2.5	14	13	13	12	9
3	26	25	24	22	20

### 3 Heat demand

Heat production is directly related to heat demand of a building. In this study, test building is assumed to be VEBIC lab, located in Vaasa, Finland. This lab serves the purpose of both industrial and academic studies, mainly related to diesel engine testing and optimization. TES supposedly charge with the exhaustion heat of this diesel engine. To find heat demand of a building, an estimated area should be known. It has been standardized by government agency depending on the building types [2]. A roughly estimated heat demand of a test building for a suitable heat pump is written as:

- Area of building = 3268 m<sup>2</sup>.
- Heating net demand = 25 – 105 kWh/m<sup>2</sup> (Laitinen et al. 2014).
- Heating demand for test building = 10.39 – 43.65 kW.
- Heat pump = 60 kW.

Energy demand of a building does not only include heating but also cooling and domestic hot water (DHW). In the above mentioned estimates, only space heating demand is taken into account. Inclusive energy demand of buildings may also be considered for a more accurate estimate [15]. The amount of energy demand vary from 25 to 232 kWh/m<sup>2</sup> depending on the category of building and

the year of construction. So smallest heating demand between the two is of the net zero energy building. For VEBIC lab type building a 60 kW heat pump was selected along with a connection to district heating system as a backup.

### 4 Heat loss in the ground

Simulation of previously mentioned system are done with multiple parameters and conditions. For example, in our case complete system may be divided into three parts, first part refers to charging of TES, second part addresses heat loss between the time of charging and discharging of TES, and third part elaborates extraction of heat energy. Simulation with all constraints and assumptions may be done simultaneously of charging and discharging but heat loss between gaps can be addressed separately. Heat loss in the ground in our case refers to the temperature change in the ground from the end of charging operation to the beginning of the extraction. Heat loss in the ground can be addressed in few ways illustrated in Fig. 8: Heat loss in TES may cause by variation of the surface temperature, air temperature from season to season can cause a huge amount of heat loss if the surface of TES is not well insulated. Heat loss in TES may cause by heat conduction in the neighboring ground, low temperature seasonal storage results in less losses compare to high temperature seasonal storage. Heat

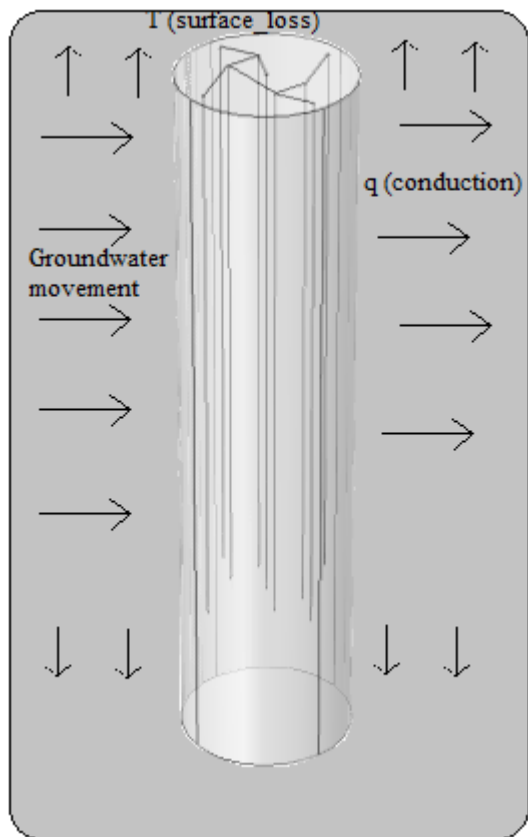


Figure 8. Heat loss in TES. Illustration of heat loss due to conduction, ground surface temperature, and groundwater movement.

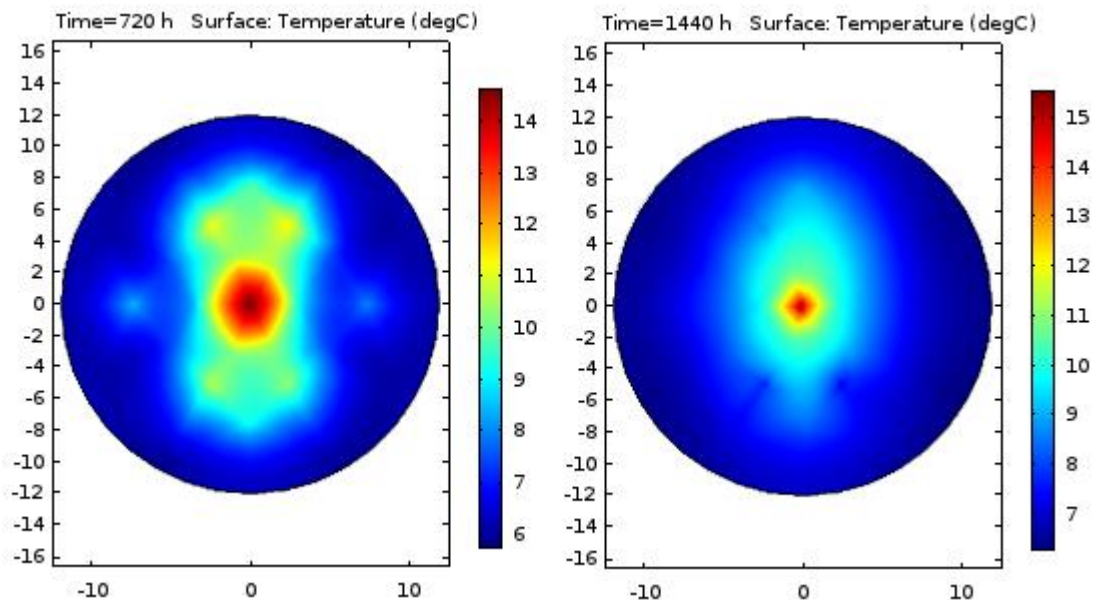


Figure 9. Ground surface temperature at the end of charging operation, temperature change in the ground surface shows the heat loss due to heat conduction in the neighboring ground within a period of one month after the end of charging TES. X and Y axes represents the geometrical length and width of TES.

loss in TES may cause by groundwater movement, [16] theoretically explained how natural groundwater movement has negligible effect in homogenous ground for steady state case. Groundwater movement has been considered problematic especially in Nordic countries, over a long period of time, a single borehole in a groundwater movement region may do no good for the purpose of extracting heat energy. TES such as our case, is a combination of nine boreholes with sufficient distance among them all. Since, velocity of natural groundwater movement in real time is small about  $10^{-6}$  meter per second, and TES is to be used as seasonally, problem of groundwater movement will not be addressed in this study. Heat loss still yet to be calculated based on the charging operation of TES. For this purpose, a simulation is made for time duration of 2 months. Variables in this simulation remain the same as in the previous ones except after one month of charging, flow rate of the fluid significantly reduced down to stop the charging process and the input signal settled down to the initial ground temperature. Ground temperature change is depicted in Fig 9. The average ground temperature change is found to be around  $1^{\circ}\text{C}$  to  $2^{\circ}\text{C}$  within the time duration of one month. It should be noted that no external signals predicting loss has been applied to illustrate the temperature change in the ground.

## 5 Heat extraction

So far, heat energy demand for a test building and the amount of heat rate injected into the TES have been calculated. Lastly, heat capacity of the ground TES with a suitable heat pump is yet to be determined. Assumptions made calculate heat capacity of the TES presented in Table 3. Heat capacity is calculated irrespective of the time domain. For a single U-shaped loop of ground heat exchanger, length of the borehole borrowed from IGSHA stated as [9]:

$$L = \frac{Q \left( \frac{COP-1}{COP} \right) (R_b + R_g F_h)}{T_g - \left( \frac{EWT_{min} + LWT_{min}}{2} \right)} \quad (2)$$

Where  $Q$  (W) is heat capacity,  $COP$  is coefficient of performance,  $L$  (m) is length of borehole,  $R$  (m.K/W) is thermal resistance,  $F_h$  is run fraction,  $T_g$  ( $^{\circ}\text{C}$ ) is temperature of ground,  $EWT_{min}$  ( $^{\circ}\text{C}$ ) is entering water temperature, and  $LWT_{min}$  ( $^{\circ}\text{C}$ ) is leaving water temperature. Ground temperature set to be after operation of one month with heat injection. Average entering and leaving water temperatures recommended to be  $0^{\circ}\text{C}$  (Laitinen et

al. 2014). Eq. (2) can be further derived to find heat capacity:

$$Q = \frac{L \left( T_g - \left( \frac{EWT_{min} + LWT_{min}}{2} \right) \right)}{\left( \frac{COP-1}{COP} \right) (R_b + R_g F_h)} \quad (3)$$

Length of the borehole, average entering and leaving water temperature, COP, run fraction, and ground temperature are usually given or may be assumed considering another close by application of the system or study of the country's geological survey. Thermal resistances of ground and borehole can be calculated as:

$$R_b = \frac{1}{SF_b k_{grout}} + \frac{\ln(D_o/D_i)}{4\pi k_p} \quad (4)$$

Where  $k_{grout}$  (W/m.K) is thermal conductivity of grout,  $k_p$  (W/m.K) is thermal conductivity of pipe,  $D$  (m) is diameter of pipe, and  $SF_b$  is dimensionless shape factor which represents the placement of pipe inside the borehole and the separation between inlet and outlet of the pipe. Thermal resistance of the ground can be calculated as:

$$R_g = \frac{\ln(D_g/D_b)}{2\pi k_g} \quad (5)$$

Where  $D_g$  (m) is diameter of the ground assumed,  $D_b$  (m) is diameter of borehole, and  $k_g$  (W/m.K) is thermal conductivity of the ground. By putting all the given values in eq. (3), a heat capacity of ground TES may be calculated with a suitable heat pump.

Heat extraction process is depicted in Fig. 10, where TES is connected to a heat pump providing heat energy to the distribution network. Heat capacity is calculated with multiple length of boreholes expressed in Fig. 11. On x-axis, number of boreholes are mentioned in which one borehole represents 250 meters of length of the borehole. Heat demand of our test case is completely met by our calculations. Ground temperature is a crucial parameter in this calculation which were kept constant for all the heat capacity calculations. In practice, it may not be constant or even similar among boreholes but continuous injection of heat energy with industrial waste storage can only increase the temperature of the ground. Heat demand of test building can be met with a series connection of four boreholes as depicted in Fig. 11. Heat pump for VEBIC lab was chosen with a heat capacity of 60 kW. Recall that, heat capacity was only calculated for space heating. Domestic hot

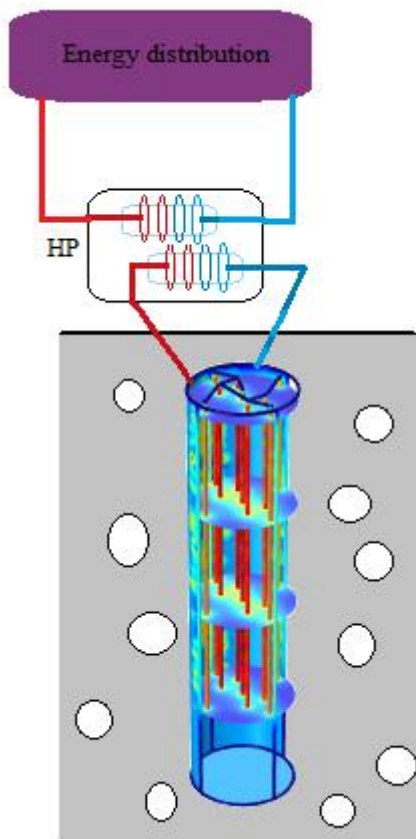


Figure 10. Heat extraction from TES in combination with a heat exchanger and distribution network, red and blue lines show the heat transfer between hot and cold fluid.

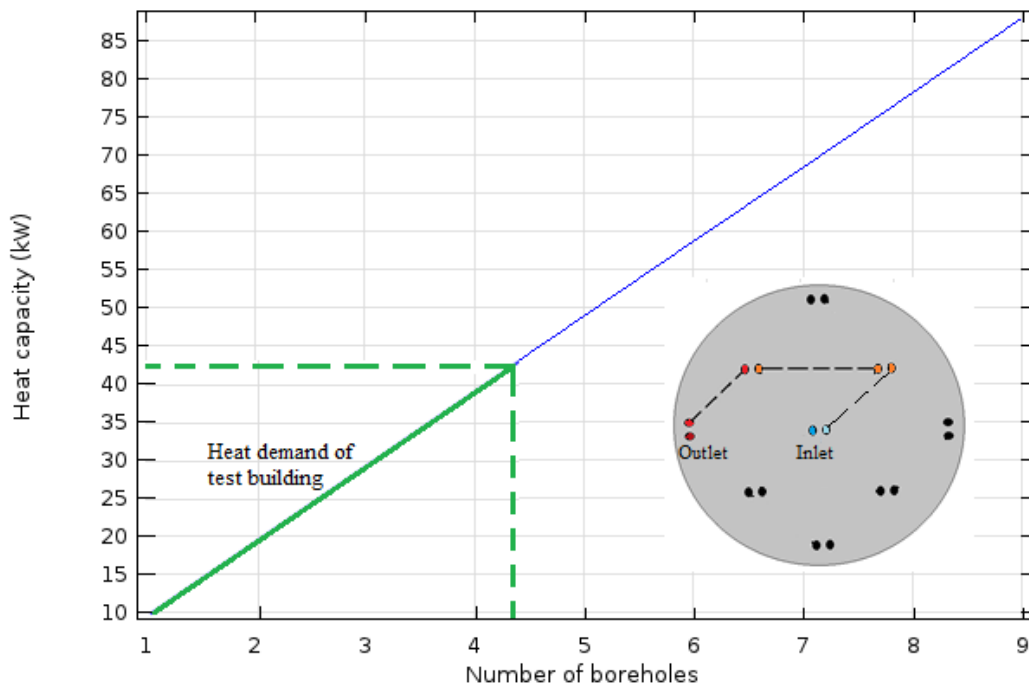


Figure 11. Heat capacity of the TES, depiction of heat demand of test building met by the given configuration, one borehole represents 250 m of depth.

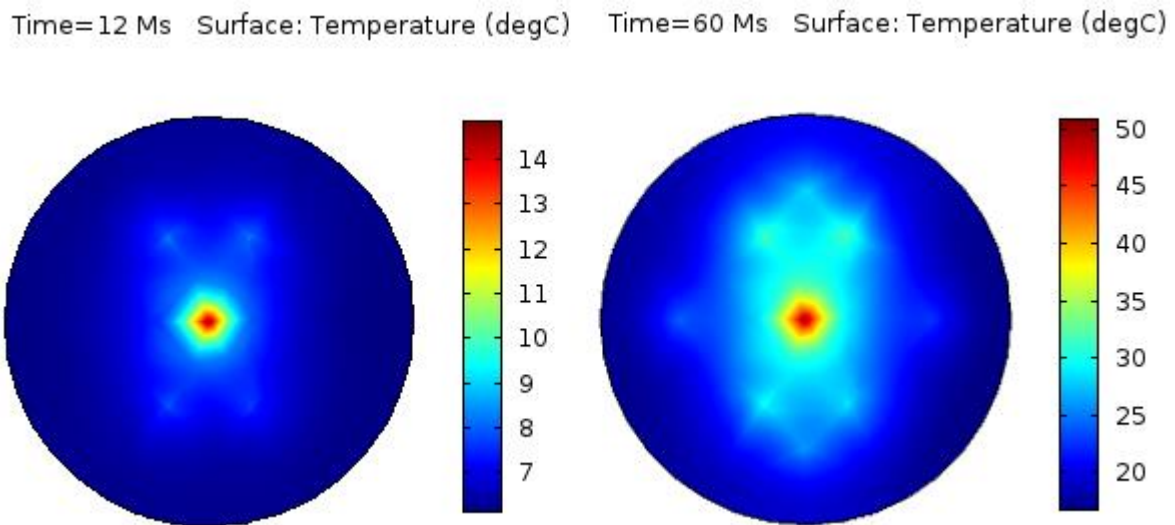


Figure 12. Charging of TES for 5 years period with the given hourly periodic input signal. Surface temperature of the TES is presented after one year on the left hand side and after five years on the right hand side.

water (DHW) was exempt from our calculation. So, it may be fairly reasonable to use a 60 kW heat pump to meet energy demand. Heat loss during and after operations were not included into the simulation using number of boreholes along with a constant ground temperature, but increase temperature of the ground due to injection was also not assumed into the calculation. A simulation was made to illustrate the rise in ground temperature in Fig. 12, in which injection operation was performed for a time period of 5 years. Ground temperature rise to an average of 35 °C after five years of injection if heat losses were ignored and no heat extraction taken into account.

Table 3. Parameters used in calculation of heat capacity

Parameter	Symbol	Value
Borehole diameter	$D_b$	140 (mm)
Pipe's outer diameter	$D_o$	40 (mm)
Pipe's inner diameter	$D_i$	35.2 (mm)
Mean temperature of source	$(EWT_{min} + LWT_{min})/2$	0 (°C)
Ground temperature	$T_g$	10 (°C)

Coefficient of performance	$COP$	4
Ground's thermal conductivity	$k_g$	3.4 (W/m·K)
Grout's thermal conductivity	$k_b$	0.57 (W/m·K)
Pipe's thermal conductivity	$k_p$	0.4 (W/m·K)

## 6 Conclusion

This study brought an analysis to use TES with an industrial waste application. Paper is divided into multiple sections in which a discussion on input signal to the TES was conducted along with the strategy of implementation. Injection process on TES was defined, configuration of borehole was selected based on the depth of TES and heat rate to the ground. Stability of the heat rate evidently suggested 250 meters depth of TES to be preferable considering the input signal in our case. Heat rate transmitted to the ground was calculated by varying flow rate of the carrier fluid. Heat energy demand was calculated for a test building case recommended by a previous government's study. Heat loss in the ground between the time duration of heat injection and heat extraction was illustrated. Heat capacity of the TES was calculated after a month of injection operation. TES capacity is enough to meet the

energy demand of test building with a configuration. Temperature rise in the ground after 5 years of operation was shown. Heat loss in the ground may need more consideration in order to find accurate values. Simultaneous simulation may result in a complex results which may be difficult to interpret, it is recommended that simplifying a complex system with less parameter may provide better results.

### Acknowledgement of funding

The authors are grateful for the funding provided by the University of Vaasa Foundation.

### References:

- [1] A. Lazzarotto, A network-based methodology for the simulation of borehole heat storage systems, *Renewable Energy*, 62 (2014) 265–275, doi:http://doi.org/10.1016/j.renene.2013.07.020.
- [2] A. Laitinen, P. Tuominen, R. Holopainen, P. Tuomaala, J. Jokisalo, L. Eskola, K. Siren, Renewable energy production of Finnish heat pumps, Final report of the SPF-project, VTT Technology 164 (2014).
- [3] B. McDaniel, D. Kosanovic, Modeling of combined heat and power plant performance with seasonal thermal energy storage, *Journal of Energy Storage* 7 (2016) 13–23, doi:http://doi.org/10.1016/j.est.2016.04.006.
- [4] C. Flynn, K. Siren, Influence of location and design on the performance of a solar district heating system equipped with borehole seasonal storage, *Renewable Energy* 81 (2015) 377–388, doi:http://doi.org/10.1016/j.renene.2015.03.036 .
- [5] D. Bauer, R. Marx, J. Nußbicker-Lux, F. Ochs, W. Heidemann, H. Müller-Steinhagen, German central solar heating plants with seasonal heat storage, *Solar Energy*, 84 (2010) 612–623, doi:http://doi.org/10.1016/j.solener.2009.05.013 .
- [6] F. M. Rad, A. S. Fung, M. A. Rosen, An integrated model for designing a solar community heating system with borehole thermal storage, *Energy for Sustainable Development* 36 (2017) 6–15, doi:http://doi.org/10.1016/j.est.2016.10.003.
- [7] F. Ruiz-Calvo, C. Montagud, Geothermics Reference data sets for validating GSHP system models and analyzing performance parameters based on a five-year operation period, *Geothermics* 51 (2014) 417–428, doi:http://doi.org/10.1016/j.geothermics.2014.03.010.
- [8] G. Engel, S. Asenbeck, R. Köll, H. Kerskes, W. Wagner, W. van Helden, Simulation of a seasonal, solar-driven sorption storage heating system, *Journal of Energy Storage*, 13 (2017) 40–47, doi:http://doi.org/10.1016/j.est.2017.06.001.
- [9] G. Narsilio, I. Johnston, A. Bidarmaghz, O. Mikhayalova, O. Kivi, R. Aditaya, Geothermal Energy: Introducing an emerging technology, International conference on advances in Civil Engineering for Sustainable Development (2014) 141–154.
- [10] H. Wang, W. Yin, E. Abdollahi, R. Lahdelma, W. Jiao, Modelling and optimization of CHP based district heating system with renewable energy production and energy storage, *Applied Energy*, 159 (2015) 401–421, doi:http://doi.org/10.1016/j.apenergy.2015.09.020.
- [11] J. Hu, An improved analytical model for vertical borehole ground heat exchanger with multiple-layer substrates and groundwater flow, *Applied Energy*, 202 (2017) 537–549, doi:http://doi.org/10.1016/j.apenergy.2017.05.152.
- [12] L. Lamarche, Mixed arrangement of multiple input-output borehole systems, *Applied Thermal Engineering*, 124 (2017) 466–476, doi:http://doi.org/10.1016/j.applthermaleng.2017.06.060.
- [13] N. Rapantova, P. Pospisil, J. Koziorek, P. Vojcinak, D. Grycz, Z. Rozehnal, Optimization of experimental operation of borehole thermal energy storage, *Applied Energy* 181 (2016) 464–476, doi:http://doi.org/10.1016/j.ap.ene.2016.08.091.
- [14] P. Kandiah, M. F. Lightstone, Geothermics Modelling of the thermal performance of a borehole field containing a large buried tank, *Geothermics* 60 (2016) 94–104,

doi:<http://doi.org/10.1016/j.geothermics.2015.12.001>.

- [15] P. Zangheri, R. Armani, M. Pietrobon, L. Pagliano, M. Fernandez Boneta, A. Müller, Heating and cooling energy demand and loads for building types in different countries of the EU, 86 (2014), Retrieved from [http://www.entranze.eu/files/downloads/D2\\_3/Heating\\_and\\_cooling\\_energy\\_demand\\_and\\_loads\\_for\\_building\\_types\\_in\\_different\\_countries\\_of\\_the\\_EU.pdf](http://www.entranze.eu/files/downloads/D2_3/Heating_and_cooling_energy_demand_and_loads_for_building_types_in_different_countries_of_the_EU.pdf).
- [16] P. Eskilson, Thermal Analysis of Heat Extraction Boreholes, Doctoral thesis, Dept. of Mathematical Physics, University of Lund, Sweden, (1987).
- [17] S. Focaccia, F. Tinti, Geothermics An innovative Borehole Heat Exchanger configuration with improved heat transfer, Geothermics 48 (2013) 93–100, doi:<http://doi.org/10.1016/j.geothermics.2013.06.003>.
- [18] T. Nuytten, B. Claessens, K. Paredis, J. Van Bael, D. Six, Flexibility of a combined heat and power system with thermal energy storage for district heating, Applied Energy, 104 (2013) 583–591, doi:<http://doi.org/10.1016/j.apenergy.2012.11.029>.
- [19] Z. M. Olfman, A. D. Woodbury, J. Bartley, Geothermics Effects of depth and material property variations on the ground temperature response to heating by a deep vertical ground heat exchanger in purely conductive media, Geothermics 51 (2014) 9–30, doi:<http://doi.org/10.1016/j.geothermics.2013.10.002>.

### List of Abbreviations

$r_g$	Radius of ground (m)
$d_g$	Distance between boreholes (m)
$L$	Depth of borehole (m)
$D$	Distance between pipes (m)
$q$	Flow rate (l/s)
$k_g$	Thermal conductivity of ground (W/m.K)
$T_0$	Initial ground temperature ( $^{\circ}$ C)

$T_{sur}$	Surface temperature of ground ( $^{\circ}$ C)
$T_g$	Boundary ground temperature ( $^{\circ}$ C)
$d_i$	Inner pipe diameter (m)
$k_p$	Thermal conductivity of pipe (W/m.K)
$Q$	Heat rate (W)
$m$	Mass flow rate (kg/s)
$c_p$	Heat capacity (J/kg.K)
$T_{in}$	Input temperature of fluid ( $^{\circ}$ C)
$T_{out}$	Output temperature of fluid ( $^{\circ}$ C)
$T_{1,2,3,4out(max)}$	Outlet temperature of the fluid ( $^{\circ}$ C)
$COP$	Coefficient of performance
$TES$	Thermal energy storage
$R_b$	Thermal resistance of borehole (m.K/W)
$R_g$	Thermal resistance of ground (m.K/W)
$F_h$	Run fraction of heat pump
$EWT_{min}$	Entering water temperature to the heat pump ( $^{\circ}$ C)
$LWT_{min}$	Leaving water temperature from the heat pump ( $^{\circ}$ C)
$SF_b$	Shape factor
$k_{grout}$	Thermal conductivity of grout (W/m.K)
$k_b$	Thermal conductivity of borehole (W/m.K)
$D_o$	Outer pipe diameter (m)
$D_i$	Inner pipe diameter (m)
$D_g$	Diameter of the ground (m)
$D_b$	Diameter of the borehole (m)